

Ga flux dependence of Er-doped GaN luminescent thin films

D. S. Lee and A. J. Steckl^{a)}

Nanoelectronics Laboratory, University of Cincinnati, Cincinnati, Ohio 45221-0030

(Received 19 October 2001; accepted for publication 27 November 2001)

Er-doped GaN thin films have been grown on (111) Si substrates with various Ga fluxes in a radio frequency plasma molecular beam epitaxy system. Visible photoluminescence (PL) and electroluminescence (EL) emission at 537/558 nm and infrared (IR) PL emission at 1.5 μm from GaN:Er films exhibited strong dependence on the Ga flux. Both visible and IR PL and visible EL increase with the Ga flux up to the stoichiometric growth condition, as determined by growth rate saturation. Beyond this condition, all luminescence levels abruptly dropped to the detection limit with increasing Ga flux. The Er concentration, measured by secondary ion mass spectroscopy and Rutherford backscattering, decreases with increasing Ga flux under N-rich growth conditions and remains constant above the stoichiometric growth condition. X-ray diffraction indicated that the crystalline quality of the GaN:Er film was improved with increasing Ga flux up to stoichiometric growth condition and then saturated. Er ions in the films grown under N-rich conditions appear much more optically active than those in the films grown under Ga-rich conditions. © 2002 American Institute of Physics. [DOI: 10.1063/1.1447318]

Rare-earth (RE)-doped GaN is being widely studied¹ for its various applications to optoelectronics and optical communications, mostly due to the characteristic 1.54 μm infrared (IR) emission from Er³⁺ ions. Much effort has been devoted to Er-doped wide band gap semiconductors after Favennec *et al.* reported² that Er³⁺ photoluminescence (PL) intensity depends strongly on both the band gap energy of the semiconductor and the host temperature. GaN has advantages over other semiconductors such as a direct band gap transition which is very important in optical applications, a large energy band gap which results in very low thermal quenching,^{3,4} and thermal and chemical robustness. Other wide band gap semiconductors used as hosts, such as II–VI compounds, are less stable than GaN and suffer from lack of charge neutrality when doped with RE³⁺ ions. The inherent robustness of GaN has been an important factor in the successful development of conventional GaN *p-n* junction light emitting diodes (LEDs) which operate by carrier recombination, as well as the electroluminescent devices (ELDs) discussed in this letter which operate by impact excitation. Since we reported⁵ the visible green emission from Er-doped GaN, our research has been focused to achieve the three primary colors from RE-doped GaN. The molecular beam epitaxy (MBE) growth process for *in situ* RE doping of GaN has resulted^{6,7} in the successful fabrication of ELDs with red, green, and blue (RGB) color emissions using Eu, Er, and Tm, respectively. We have also achieved⁸ RGB colors in electroluminescence (EL) emission from RE-doped GaN films grown at nominally room temperature using same set of rare-earth elements. Throughout our studies we have observed that RE optical emission from GaN films is a strong function of the Ga flux during growth. Considering that GaN crystallinity and intrinsic luminescence are known to be a strong function of Ga flux during growth, it is clear that the RE-related emission also strongly depends on the crystallin-

ity of the GaN host. This indicates that the effect of the Ga flux on RE emission needs to be understood and optimized in order to enhance optical activity in RE-doped GaN films. In this letter, we report on the effect of Ga flux on optical and structural properties of RE-doped GaN films by using Er-doped GaN.

GaN films were grown on *p*-type (111) Si substrates by MBE with a Ga elemental source and a nitrogen plasma source. Er doping was performed *in situ* during growth from a solid source. AlN buffer layers were first grown for 5 min. GaN:Er layers were then grown typically for 1 h. Ring-shaped Schottky diodes were fabricated for EL measurements using indium tin oxide sputtering and a lift-off process. The area of the electrode is $7.65 \times 10^{-4} \text{ cm}^2$ and its detailed structure is reported elsewhere.⁹

Er-doped GaN films were grown with various Ga cell temperatures from 850 to 945 °C, which resulted in beam equivalent pressures (BEP) from $\sim 1.5 \times 10^{-7}$ to $\sim 9.0 \times 10^{-7}$ Torr. It is well accepted that Ga flux is critical to GaN crystalline quality and good crystalline GaN is usually grown under a slightly Ga-rich¹⁰ growth condition. All other growth parameters were fixed: 600 °C for growth temperature, 860 °C for Er cell temperature, 1.2 sccm for nitrogen flow, and 300 W for plasma power.

GaN:Er film thickness, as measured by scanning electron microscopy, is plotted in Fig. 1 versus Ga flux specified by BEP in the MBE system. The film thickness increases with Ga flux up to $(4.5\text{--}5.0) \times 10^{-7}$ Torr, after which it is constant. The stoichiometric growth condition is usually determined¹⁰ as the Ga flux at which thickness (or equivalent growth rate) saturation starts. In this set of samples stoichiometry appears to be located between 4.5×10^{-7} and 5.0×10^{-7} Torr (shaded region in the plot). The saturated growth rate was $\sim 0.5 \mu\text{m/h}$. The same shaded region is also drawn in all the following figures for better comparison.

Secondary ion mass spectroscopy (SIMS) and Rutherford backscattering (RBS) were performed to evaluate the

^{a)}Electronic mail: a.steckl@uc.edu

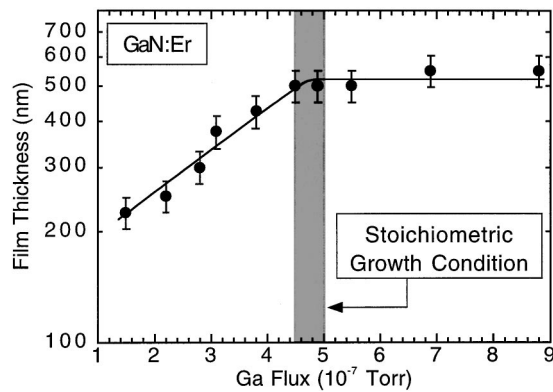


FIG. 1. GaN:Er film thickness vs Ga flux used during growth. Stoichiometric growth condition was determined by film thickness saturation to be between $\sim 4.5 \times 10^{-7}$ and $\sim 5.0 \times 10^{-7}$ Torr in Ga beam equivalent pressure (BEP).

absolute Er concentration in the GaN:Er films grown with various Ga fluxes. In spite of using the same Er cell temperature of 860 °C, Er concentration varied significantly with different Ga flux. As shown in Fig. 2, the Er concentration decreases almost exponentially with Ga flux up to the stoichiometric growth region ($\sim 4.5 \times 10^{-7}$ Torr) and then stays constant. Er concentration saturation appears almost complementary to that of growth rate. This is consistent with previously reported¹¹ results for GaN:Er films grown under different conditions. Two possible explanations for the variation in Er incorporation with Ga flux are: (1) the lower GaN:Er film growth rate at low Ga flux allows the incorporation of a larger concentration of Er; (2) site competition between Er and Ga atomic species results in a decreased incorporation of Er atoms when the Ga supply is increased. RBS channeling was performed on four samples grown with Ga BEPs between 2.0 and 7.0×10^{-7} Torr in order to investigate these films more thoroughly. The sample grown with the Ga-rich condition of 7.0×10^{-7} Torr of Ga showed that over 95% of Er atoms occupy the same lattice locations as Ga atoms. The films grown with lower Ga flux were not sufficiently crystalline to observe RBS channeling. However, considering that even at high Ga flux the Er atoms are incorporated into the Ga sublattice, it is very likely that the same is the case at the lower Ga flux values.

X-ray diffraction (XRD) was performed to investigate the structure of these films. Figure 3 shows the (0002) peak

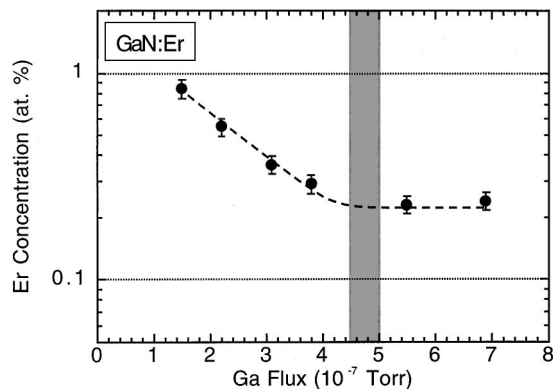


FIG. 2. Er concentration measured by SIMS and RBS as a function of Ga flux. Er cell temperature was fixed at 860 °C.

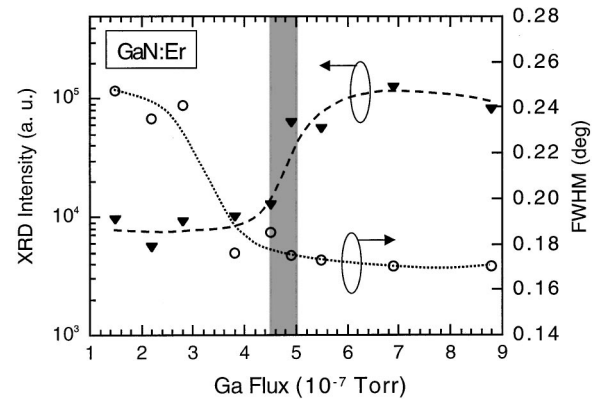


FIG. 3. Intensity of (0002) hexagonal GaN XRD peak in GaN:Er films as a function of Ga flux. The peak intensity and its linewidth show a complementary behavior vs the Ga flux, with a saturation in crystallinity beyond the stoichiometric growth condition.

intensity of hexagonal GaN observed at $2\theta = 34.5^\circ$ and its full width at half maximum (FWHM) as a function of Ga flux. The x-ray peak intensity was normalized to the film thickness for each sample. The peak intensity at first is nearly constant with Ga BEP. It increases fairly abruptly just before the stoichiometric regime and then starts to be saturated at around $\sim 5.0 \times 10^{-7}$ Torr. The FWHM shows a complementary behavior, reaching a minimum at around the same Ga BEP. The crystalline structure in terms of XRD reaches its maximum at just after the determined stoichiometric growth condition. A similar trend was observed by *in situ* reflection high energy electron diffraction (RHEED) from the sample surface. At low values of Ga BEP, the RHEED pattern indicated amorphous material. A spotty pattern with hexagonal symmetry is observed in the N-rich range up to the stoichiometric condition. In the slightly Ga-rich range the RHEED pattern is mainly streaky indicating two-dimensional growth and an improvement in crystallinity.

Photoluminescence (PL) was carried out at room temperature by above-band gap excitation using a HeCd (325 nm) laser. The visible emission from GaN:Er has two characteristic green peaks at 537 and 558 nm, which are caused by two $4f-4f$ Er³⁺ inner shell transitions: ${}^2H_{11/2} \rightarrow {}^4I_{15/2}$ and ${}^4S_{3/2} \rightarrow {}^4I_{15/2}$, respectively. There is also near-infrared (IR) emission due to the ${}^4I_{13/2} \rightarrow {}^4I_{15/2}$ transition, which has been widely studied because of the applications to optoelectronics and optical communications using silica-based optical fibers. Figure 4 shows the visible and IR PL intensity from Er³⁺ ions, as well as ultraviolet (UV) band edge emission of the GaN host, as a function of Ga flux. Visible and IR data were normalized to the incorporated Er concentration as plotted in Fig. 2. Two different detectors were used for the UV/visible and infrared measurement. Therefore only the UV and visible emission can be directly compared. The GaN band edge emission at 369 nm was much stronger in samples grown under Ga-rich conditions, consistent with the results of other groups. Reduced intensity at the highest Ga flux is due to Ga droplets formed on the GaN surface, which act as a screen for the emitted light. The PL from Er³⁺ ions exhibits a very interesting behavior. Both visible and IR emission increased with Ga flux up to the stoichiometric growth condition followed by a very abrupt reduction to the detection limit of the measurement.

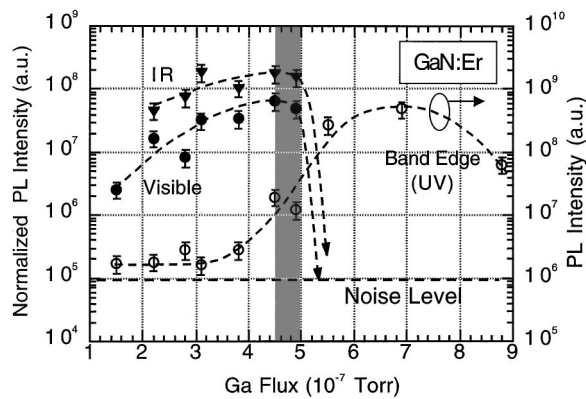


FIG. 4. PL intensity from GaN:Er films vs Ga flux. GaN band edge emission at 369 nm increases with Ga flux and has a maximum in the Ga-rich growth regime. The PL intensity of visible and IR emission from Er^{3+} ions (normalized by the incorporated Er concentration) increases with Ga flux and then drops abruptly to the detection limit near stoichiometric growth condition.

For comparison of EL intensity from devices fabricated with various Ga fluxes, we use the brightness normalized by current flow versus voltage, defined as BIV. The BIV is a more useful indicator of relative brightness potential since the non-current-normalized EL brightness is influenced by many factors associated with film quality and device fabrication. Figure 5 shows maximum visible BIV values from each sample grown with a different Ga flux. The observed dependence is very similar to that of PL vs. Ga flux except that the BIV peaked at slightly less Ga flux than the PL. The strongest BIV was observed from the sample grown under slightly N-rich condition, while for growth above the stoichiometric condition, the BIV dropped rapidly to the detection limit of the measurement.

The reason for the quenching of the Er-based emission near the stoichiometric growth condition is probably due to the increasing efficiency of the intrinsic band-edge emission

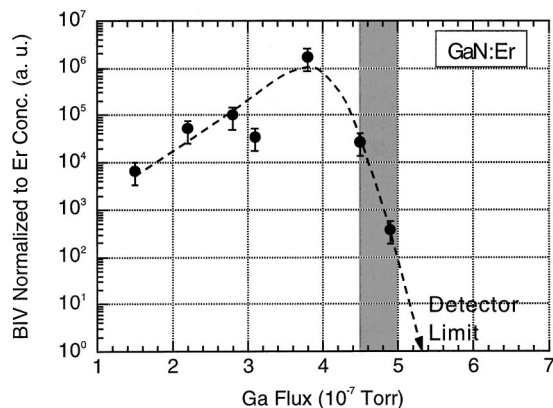


FIG. 5. Maximum current-normalized visible EL brightness (BIV) vs Ga flux. The BIV signal is also normalized to the Er concentration incorporated at each Ga flux condition. BIV increases with Ga flux and then drops abruptly near stoichiometric growth condition. Strongest BIV was obtained under slightly N-rich condition.

in the GaN host, which then provides a faster relaxation path for excited carriers. It is also possible, but unlikely, that the lattice location (and hence optical properties) of Er atoms incorporated at low to moderate Ga flux is different from the Ga sublattice location determined for high Ga flux.

In summary, we have grown Er-doped GaN films with various Ga fluxes and investigated their optical and structural properties. Ga flux for the stoichiometric growth condition was determined by the onset of thickness (or equivalent growth rate) saturation at a value of $\sim 0.5 \mu\text{m/h}$. Er concentration measured by SIMS and RBS decreased with increasing Ga flux up to the stoichiometric growth condition and then stayed constant. Crystalline quality in terms of XRD also improved with increasing Ga flux and then saturated near the stoichiometric Ga flux condition. Er-related PL and EL emission intensity dependence on Ga flux exhibited a very interesting phenomenon. Under N-rich conditions, the intensity became stronger with increasing Ga flux. Then in the vicinity of the stoichiometric Ga flux condition, both PL and EL intensity was reduced abruptly to the detection limit for both visible and IR emission. This leads us to conclude that Er ions in GaN:Er films were more optically active when the films were grown under N-rich conditions than Ga-rich conditions. The optimum growth condition of Er optical activity is under slightly N-rich flux near the stoichiometric region. Under these growth conditions, the resulting GaN crystallinity is high enough for efficient Er excitation but the competition from intrinsic carrier recombination is not yet very strong. From this study we also conclude that while rare-earth-based optical emission (PL, EL) does strongly depend on the crystallinity of the GaN host, the highest quality crystalline GaN is not necessary to achieve the strongest emission from rare-earth-doped GaN films.

This work was supported by ARO Grant No. DAAD19-99-1-0348. Equipment support was provided by an ARO URI grant and the Ohio Materials Network. The authors are pleased to acknowledge the support of M. Gerhold and J. Zavada.

- ¹A. J. Steckl and J. M. Zavada, *MRS Bull.* **24**, 33 (1999).
- ²P. N. Favennec, H. L'Haridon, D. Moutonnet, M. Salvi, and Y. LeGuillou, *Electron. Lett.* **25**, 718 (1989).
- ³M. Thaik, U. Hommerich, R. N. Schwartz, R. G. Wilson, and J. M. Zavada, *Appl. Phys. Lett.* **71**, 2641 (1997).
- ⁴J. M. Zavada, M. Thaik, U. Hommerich, J. D. MacKenzie, C. R. Abernathy, and S. J. Pearton, *J. Alloys Compd.* **300-301**, 207 (2000).
- ⁵A. J. Steckl and R. Birkhahn, *Appl. Phys. Lett.* **73**, 1700 (1998).
- ⁶A. J. Steckl, J. Heikenfeld, M. Garter, R. Birkhahn, and D. S. Lee, *Compound Semicond.* **6**, 48 (2000).
- ⁷A. J. Steckl, J. Heikenfeld, D. S. Lee, and M. Garter, *Mater. Sci. Eng., B* **81**, 97 (2001).
- ⁸D. S. Lee and A. J. Steckl, *Appl. Phys. Lett.* **79**, 1962 (2001).
- ⁹D. S. Lee, J. Heikenfeld, R. Birkhahn, M. Garter, B. K. Lee, and A. J. Steckl, *Appl. Phys. Lett.* **76**, 1525 (2000).
- ¹⁰E. Calleja, M. A. Sanchez-Garcia, F. J. Sanchez, F. Calle, F. B. Naranjo, E. Munoz, U. Jahn, and K. Ploog, *Phys. Rev. B* **62**, 16826 (2000).
- ¹¹K. Lorenz, R. Vianden, R. Birkhahn, A. J. Steckl, M. F. da Silva, J. C. Soares, and E. Alves, *Nucl. Instrum. Methods Phys. Res. B* **161-163**, 946 (2000).